J Biomol NMR (2009) 44:1–11
DOI 10.1007/s10858-009-9311-5

ARTICLE

NMR investigations on residue level unfolding thermodynamics in DLC8 dimer by temperature dependent native state hydrogen exchange

P. M. Krishna Mohan · Swagata Chakraborty · Ramakrishna V. Hosur

Received: 12 January 2009 / Accepted: 26 February 2009 / Published online: 24 March 2009

Abstract Understanding protein stability at residue level detail in the native state ensemble of a protein is crucial to understanding its biological function. At the same time, deriving thermodynamic parameters using conventional spectroscopic and calorimetric techniques remains a major challenge for some proteins due to protein aggregation and irreversibility of denaturation at higher temperature values. In this regard, we describe here the NMR investigations on the conformational stabilities and related thermodynamic parameters such as local unfolding enthalpies, heat capacities and transition midpoints in DLC8 dimer, by using temperature dependent native state hydrogen exchange; this protein aggregates at high (>65°C) temperatures. The stability (free energy) of the native state was found to vary substantially with temperature at every residue. Significant differences were found in the thermodynamic parameters at individual residue sites indicating that the local environments in the protein structure would respond differently to external perturbations; this reflects on plasticity differences in different regions of the protein. Further, comparison of this data with similar data obtained from GdnHCl dependent native state hydrogen exchange indicated many similarities at residue level, suggesting that local unfolding transitions may be similar in both the cases. This has implications for the folding/unfolding mechanisms of the protein.

Keywords Dynein light chain protein · Nuclear magnetic resonance · Native state hydrogen exchange · Thermal stability · Unfolding energetics

Introduction

Proteins perform important tasks in all biological systems, and they do so in their functional state, called the native state. This native conformation is marginally stabilized in a balancing act of various opposing forces. The major stabilizing forces include the hydrophobic effect and hydrogen bonding while conformational entropy favors the unfolded state (Dill 1990; Honig 1999; Kauzmann 1959; Pace et al. 1996; Rose and Wolfenden 1993). The forces stabilizing the native state outweigh the disruptive forces marginally in a folded protein, in the range of 5–15 kcal/mol (Pace 1975). The balance of these forces contributes to the conformational stability of a protein and is defined thermodynamically as the change in free energy (ΔG) in going from the native state to the unfolded state. Protein stability measurements have remained important for over several decades owing to the central role these macromolecules play in maintaining life and their involvement in many diseases affecting humans. Studies on protein stability explore the sequence–structure–stability relationships and the stability is usually determined from equilibrium denaturation experiments. This can be achieved by perturbing the native state using temperature, pH or chemical denaturants (urea, GdnHCl) and systematically following the denaturation process by calorimetric and/or spectroscopic probes (Lopez and Makhatadze 2002; Pace 1986). Among the most common denaturants temperature occupies a unique role as a perturbant as the temperature dependence of equilibrium between different conformational

Electronic supplementary material The online version of this article (doi:10.1007/s10858-009-9311-5) contains supplementary material, which is available to authorized users.

P. M. Krishna Mohan · S. Chakraborty · R. V. Hosur (✉)
Department of Chemical Sciences, Tata Institute of Fundamental Research, Homi Bhabha Road, Mumbai 400 005, India
e-mail: hosur@tifr.res.in

species provides an access to the enthalpy, entropy, and heat capacity components of the Gibbs free energy (Becktel and Schellman 1987). However, thermal stability measurements on some protein systems by the traditional calorimetric and optical spectroscopic tools are severely hampered due to their differential stability behaviors such as irreversibility of unfolding process, protein aggregation etc.

Hydrogen/deuterium exchange (HX) monitored by NMR spectroscopy is a versatile probe to measure the protein stability at residue level and to detect the intermediates present in the folding transition (Bai et al. 1995; Chamberlain and Marqusee 1997; Dyson and Wright 1996; Krishna et al. 2004; Mukherjee et al. 2007). Although, HX measurement can be done over a wider range of schemes, the native-state HX method (NHX) has its own advantage. Since, under native conditions, though proteins exist predominantly in their native states according to thermodynamic principles, low populations of partially folded intermediate state(s) and fully unfolded state can also exist in equilibrium (Chu et al. 2002; Hoang et al. 2002; Maity et al. 2005; Rumbley et al. 2001). NHX takes the advantage of these infinitesimally populated higher energy states, for the native state is the H/D exchange incompetent state with regard to the majority of the slowly exchanging amide protons (Chi et al. 2002; Rumbley et al. 2001). Further, NHX experiments as a function of temperature yield complete thermodynamic picture of the protein molecule at residue level detail and this reflects on plasticity differences in different regions of the protein. Besides, as these are performed in the native state, they overcome the undesirable behavior of proteins such as aggregation. In this context, we present here insights into thermal unfolding characteristics of dynein light chain protein (DLC8), the smallest (10.3 kDa, 89 residues) and the highly conserved light chain of the dynein motor complex.

DLC8 exists as a homo dimer at physiological pH and a monomer at pH 3 (Barbar et al. 2001; Mohan et al. 2006). DLC8 is functional only in its dimeric form. The DLC8 dimer consists of two α-helices (α1, residues 15–31; α2, residues 35–50) and 5 β-strands (β1, residues 6–11; β2, residues 54–59; β3, residues 62–67; β4, residues 72–78 and β5, residues 81–87) (Liang et al. 1999). DLC8 interacts with proteins of diverse biological functions (Fuhrmann et al. 2002; Jaffrey and Snyder 1996; Lo et al. 2005; Puthalakath et al. 2001; Vadlamudi et al. 2004). Hence, it was presumed that DLC8 acts as a cargo adaptor in the dynein complex to transport various organelles. Unfolding studies on DLC8 dimer with GdnHCl suggested that the folding energy landscape comprises of intermediates (Mohan et al. 2009a; Mohan and Hosur 2008b). However, thermal unfolding behavior of the molecule is not known yet due to the formation of soluble and insoluble aggregates of the dimeric molecule at higher temperatures (>338 K) (Barbar et al. 2001). Hence, in the present study we report the thermodynamics of residue level unfolding in DLC8 dimer using temperature dependent native state hydrogen exchange analysis.

Materials and methods

Theory of hydrogen exchange

The hydrogen exchange process of backbone protons can be considered as a two state process (Hvidt and Nielsen 1966; Linderstrøm-Lang 1958), as shown in Eq. (1). The amide hydrogens are either non-exchangeable in the protected state (NH_{closed}) or susceptible to exchange in some transiently open state (NH_{open}). The general property of the transition NH_{closed} to NH_{open} is that it exposes the amide proton to the solvent. Such exposure may result from fluctuations in local structure in the folded protein, or from cooperative unfolding of either the whole protein or major parts of it.

$$NH_{closed} \underset{k_{cl}}{\overset{k_{op}}{\rightleftharpoons}} NH_{open} \xrightarrow{k_{rc}} \text{Exchanged} \tag{1}$$

where k_{op} is the opening rate, k_{cl} is the closing rate and k_{rc} is the intrinsic exchange rate of the amide protons. Under steady-state conditions, the exchange rate k_{obs} calculated from the above reaction scheme (1) is given by Eq. (2) (Hvidt and Nielsen 1966; Linderstrøm-Lang 1958).

$$k_{obs} = \frac{k_{op}k_{rc}}{k_{op} + k_{cl} + k_{rc}} \tag{2}$$

Under native conditions, where $k_{op} \ll k_{cl}$, the observed exchange rate (k_{obs}) can be written as follows (Hvidt and Nielsen 1966):

$$k_{obs} = \frac{k_{op}k_{rc}}{k_{cl} + k_{rc}} \tag{3}$$

Under EX2 (bimolecular exchange) conditions where $k_{cl} \gg k_{rc}$ (low pH and temperature), the exchange rate becomes

$$k_{obs} = k_{rc}\left(\frac{k_{op}}{k_{cl}}\right) \tag{4}$$

The stabilization free energy of the protecting structure can thus be calculated as

$$\Delta G_{HX} = -RT \ln\left(\frac{k_{op}}{k_{cl}}\right) = -RT \ln K_{op} = -RT \ln\left(\frac{k_{obs}}{k_{rc}}\right) \tag{5}$$

where R is the universal gas constant, T is the absolute temperature and K_{op} is the equilibrium constant of unfolding.

The rate contribution for a given NH may come from both local (l) and global (g) opening events (Bai et al. 1994), so k_{obs} and ΔG_{HX} can be calculated according to Eqs. 6 and 7 respectively. However, limited structural fluctuations (local fluctuations) will have low sensitivity to temperature compared to global unfolding which are more sensitive.

$$k_{obs} = k_{obs}(l) + k_{obs}(g) = [K_{op}(l) + K_{op}(g)]k_{rc} \quad (6)$$

$$\Delta G_{HX} = -RT \ln[K_{op}(l) + K_{op}(g)] \quad (7)$$

The change in free energy for protein unfolding $\Delta G(T)$ as a function of temperature (T) for a two state process can be best described by the modified Gibbs–Helmholtz equation as shown in Eq. (8) (Brorsson et al. 2004; Shih et al. 1995).

$$\Delta G(T) = \Delta H_m\left(1 - \frac{T}{T_m}\right) + \Delta C_p\left(T - T_m - T\ln\left(\frac{T}{T_m}\right)\right) \quad (8)$$

where ΔH_m, T_m and ΔC_p correspond to enthalpic change at mid point of transition, temperature at midpoint of transition and heat capacity changes, respectively. The parameter ΔC_p, which determines the curvature of the plot of ΔG versus T, is related to the hydrophobic contribution to protein stability, and in general to the change in solvent accessible hydrophobic surface associated with the transition (Privalov and Khechinashvili 1974).

Thus, from the HX experiments the free energy changes for the hydrogen-deuterium exchange can be determined and then by measuring these as a function of temperature in the range where the protein remains in the native state ensemble, the other thermodynamic parameters, namely, enthalpy change (ΔH_m) and heat capacity change (ΔC_p) can be estimated by fitting the data to Eq. 8.

Now, as mentioned before, amide protons undergo exchange by two mechanisms: (1) by a global unfolding mechanism (where $\Delta C_p \neq 0$), and (2) by local fluctuations. When both the mechanisms contribute to the exchange process the free energy will have two contributions (as per Eq. 7):

$$\Delta G_{HX}(T) = -RT \ln[\exp(-\Delta G(g)/RT) + \exp(-\Delta G(l)/RT)] \quad (9)$$

where $\Delta G(g)$ and $\Delta G(l)$ are the free energies for global and local unfolding phenomenon and can be expressed individually as shown in Eq. (8). Accordingly, there will also be separate contributions to enthalpy and heat capacity changes. However, for the local fluctuation case, $\Delta C_p(l)$ is expected to be zero. In general, it is not possible to estimate the two contributions separately, and one gets only one number for each residue. Nonetheless, it may be possible to indicate the major contributor on the basis of comparison of free energies to those derived from optical measurements. When the two free energies are similar in magnitude, global unfolding is the major contributor, and when the free energy derived from HX is much smaller than that derived from optical measurements, local fluctuation/unfolding is the major contributor.

In the above some caution is warranted in the interpretation of the results. This concerns the validity of the two-state assumption in the extraction of the exchange rates from the HX data. As stated earlier, hydrogen exchange occurs from the 'open' state which can be created either by local fluctuations or from some unfolding processes. In the former case, the two-state assumption for analyzing the exchange rates (Eq. 8) would be a good description. In the latter case if the unfolding process that leads to a state that is sufficiently capable of undergoing exchange, is cooperative, then also the two-state analysis would be a reasonable description for the exchange. However, if the unfolding required for exchange is a global event with possibility of intermediates, then the analysis of the exchange data would be more complicated. The complication here is that one does not know how much unfolding is required for the creation of the exchange-competent open state. The results from the optical studies would be very gross and would not be uniformly applicable to every residue. Thus the two-state analysis for such situations has limitations. However, it is still useful for qualitative comparisons.

Protein expression and purification

DLC8 was expressed and purified as described elsewhere (Krishna Mohan et al. 2008; Mohan et al. 2006).

NMR spectroscopy

NMR sample

For NMR studies the protein purified as described above was concentrated to ~1.2 mM (20 mM Tris, 400 mM NaCl, 2 mM DTT, pH 7). Although, DLC8 behaves very well at low salt concentrations, the protein is relatively more stable at high salt concentrations (~400 mM NaCl) without any precipitation occurring over a broad range of temperatures (277 to 320 K) and for long time periods (maximum 5–6 months). The final volume in all the samples was ~550 µl (90% H_2O + 10% D_2O) for reference spectra and 100% D_2O for those used to monitor HX phenomenon.

NMR data acquisition

All the NMR experiments were recorded using a triple channel Varian Unity-plus 600 MHz NMR spectrometer

equipped with pulse-shaping and pulse field gradient capabilities. Sensitivity enhanced 2D [^{15}N–^{1}H] heteronuclear single quantum correlation spectra (HSQC) of DLC8 dimer were recorded with the ^{1}H offset placed on H_2O resonance at 4.84 ppm and ^{15}N offset at 119 ppm (at 293 K). ^{1}H chemical shifts were calibrated relative to 2,2-dimethyl-2-silapentane-5-sulfonate (DSS). During the course of all experiments, the protein samples were found to be stable and did not precipitate or degrade with time.

Hydrogen exchange studies

The protein samples were lyophilized after adjusting the pH of the solution to 7.0 by considering the temperature into account. HX was initiated by dissolving the lyophilized samples in D_2O. Lyophylization itself did not have any adverse effect on the protein sample. The HX experiments were carried out under the sub-denaturing conditions (Krishna Mohan et al. 2008) at nine different temperatures. The temperatures used were 277, 283, 288, 293, 298, 303, 308, 313 and 318 K. The samples were loaded on a pre-tuned and pre-shimmed NMR spectrometer and a series of [^{15}N–^{1}H] HSQC were recorded at different time intervals ($\sim$for 2 to 4 months) depending on the rate of decay. Each [^{15}N–^{1}H] HSQC was recorded for a period of 13 min and consisted of 80 complex increments in the indirect ^{15}N dimension.

NMR data processing and analysis

All the data were processed using FELIX on a Silicon Graphic, Inc. work station. Prior to Fourier transformation and zero-filling, data was apodized with a sine-squared weighting function shifted by 60° in both dimensions. After zero filling and Fourier transformation the final matrix had 4,096, 1,024 points, respectively, along F_2, F_1 dimensions. The HX rates of individual $^{1}H^{N}$ in DLC8 dimer were measured by monitoring the $^{1}H^{N}$ decays by integrating the volumes of the peaks. The decays of the individual peak volumes were fitted to single exponential decay functions to obtain k_{obs}, the first order decay constant. K_{op} was then calculated using $K_{op} = (k_{obs}/k_{rc})$, where k_{rc} is theoretically determined for a residue in a specific tripeptide context (Bai et al. 1993). The free energy of HX (ΔG_{HX}) was obtained using Eq. (5). Here, we wish to be cautious and mention that k_{rc} values of Bai et al. (1993) represent an oversimplification. These values can actually be different from those derived from peptides and can be different for the open state at different residue sites depending upon the local structures. These structures will tend to slow down k_{rc} compared to what it would be for short unstructured peptides as reported by Bai et al. (1993). Thus, for a protein one would only get some bounds for the estimated free energies if we use the k_{rc} derived from short peptides. Since k_{rc} appears in the denominator in the equation for free energy calculation (Eq. 5), the estimated free energy values using the k_{rc} from Bai et al. would be the lower limits. The thermodynamic parameters (ΔH_m, T_m and ΔC_p) were calculated by fitting the free energy of HX (ΔG_{HX}) to temperature using Eq. (8).

Resonance assignments

The backbone resonance assignment in the DLC8 dimer at pH 7 was reported earlier (Krishna Mohan et al. 2008; Mohan et al. 2006). The HSQC spectra at all the temperatures studied are very similar so that transfer of assignment was readily possible by following the peak shifts.

Results

Thermal stability of DLC8 dimer

Barbar et al. (2001) reported that the thermal denaturation of DLC8 dimer is not a reversible process and denaturation at a temperature of about 338 K results in the formation of soluble and insoluble aggregates. Our thermal unfolding experiments using circular dichroism and NMR spectroscopy on DLC8 dimer corroborate those results. Further, we observed that DLC8 dimer was completely stable up to a temperature of 320 K and existed in its native conformation [Fig. 1, reference (Krishna Mohan et al. 2008)]. Hence, in the present study we used the temperature range 277–318 K to explore the thermal unfolding energetics of DLC8 dimer.

Native-state hydrogen exchange studies on DLC8 dimer

Measurement of exchange rates and free energy of stabilization

Native-state hydrogen exchange (HX) technique is one of the most powerful techniques to probe the details of a protein's energy landscape. To understand the thermodynamics of unfolding at the residue level and the nature of the energy landscape of DLC8 dimer, we performed native state hydrogen exchange experiments at pH 7 as described in "Materials and methods". Our recent pH dependent NHX results (Mohan et al. 2009a) suggested that under these experimental conditions the closure kinetic constant is much larger than the exchange rate ($k_{cl} \gg k_{rc}$) and hence the protein remains in the EX2 regime, thereby providing thermodynamic information. NHX studies were carried out

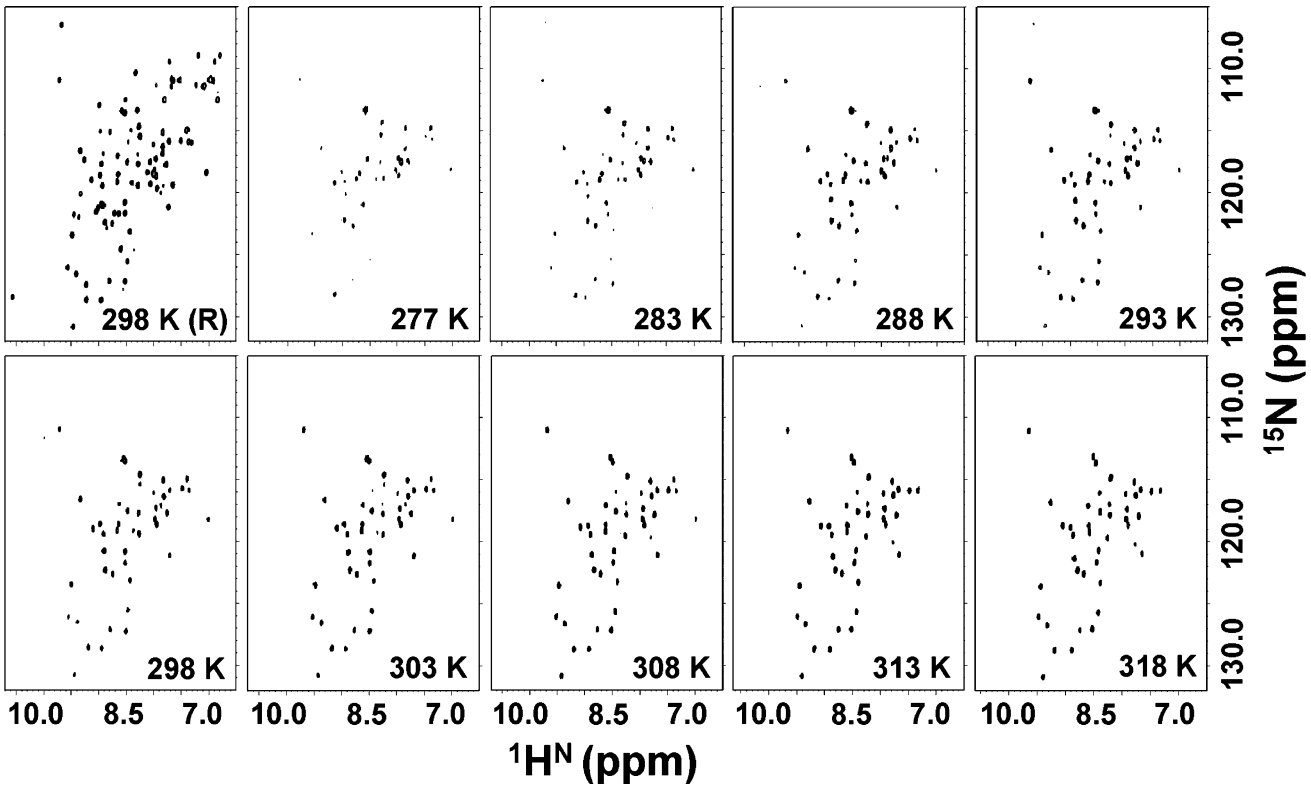

Fig. 1 The ^{1}H–^{15}N HSQC spectra of the DLC8 dimer at pH 7.0; the extreme *top left* spectrum is recorded at 298 K before adding D_2O (as a reference). All the remaining spectra are recorded 8 min after adding D_2O at various temperatures between 277 and 318 K as marked inside the *individual panels*. The appearance of more intensity of the peaks at higher temperatures in the initial HX-HSQC spectra (303–318 K) is due to the temperature induced narrowing of line widths

by recording a series of HSQC spectra at regular intervals of time for around 4 months (maximum) at nine different temperatures in the temperature range of 277–318 K. The HX analysis indicated that at all the measured temperatures the protein remained in the EX2 regime. The initial HX-HSQC spectra of the protein at all the temperature values are shown in Fig. 1. The initial HSQC spectrum was recorded 8 min (dead time) after adding D_2O. From the time dependent measurements, the decay profiles of about 50 peaks could be monitored (summation of all the peaks appeared from 288 to 308 K). The HSQC spectrum of DLC8 dimer (in H_2O) shows all the 88 amide-proton correlations (DLC8 contains one proline out of total 89 amino acids). Hence, the remaining 38 peaks which disappeared within the dead time indicate that these residues are highly accessible to solvent and are thereby easily exchangeable. Almost all of these either belong to the N- or C-terminal of the protein, or to the interconnecting loops between secondary structures. At all the measured temperatures we followed the intensity decays of all the residues for 4 months of the exchange period. These decays were fitted to single exponential functions to obtain the first order rate constants, k_{obs}. Then, we calculated the stabilization free energies (ΔG_{HX}) using Eq. (5) mentioned in materials and methods for all the residues whose rate constants were obtained.

Calculation of enthalpy changes and heat capacities

The residue-specific stabilization free energies (ΔG_{HX}) of DLC8 dimer obtained at different temperatures (Table S1 in Supplementary material) were plotted against temperature and fitted using the modified Gibbs–Helmholtz equation (Eq. 8) to obtain the thermodynamic parameters. The temperature dependent stabilization free energy behavior for four residues is shown in Fig. 2 for illustration and all the residue-specific parameters thus obtained are given in Table 1. The residue-specific summary of the enthalpy at the midpoint of transition (ΔH_m) and change in heat capacity (ΔC_p) of DLC8 dimer are shown in Fig. 3. Table 1 contains the thermodynamic information for 37 residues out of the 50 residues which appeared in the HX-HSQC spectra (includes all temperatures). The unfolding energetics of remaining 13 residues have not been obtained either due to too fast or too slow decay rates in the measured temperature range. Residues K44, I83, L84 and F86 had not decayed even at 303 K indicating very high stabilization energies. Residues H55 and I57 though decayed

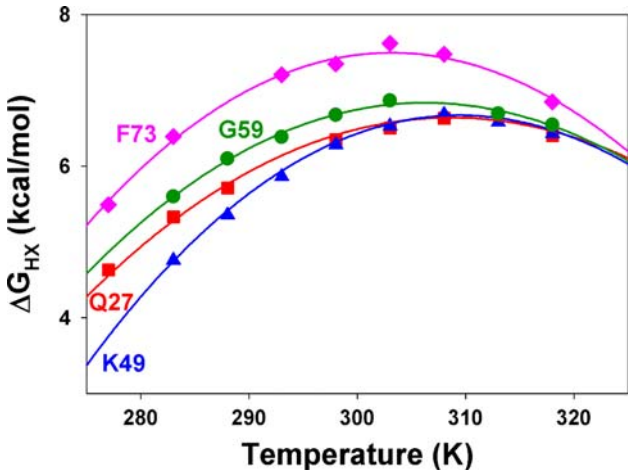

Fig. 2 Illustrative examples for four representative backbone amide protons showing the temperature dependence of the free energy of hydrogen exchange (or) stabilization free energy (ΔG_{HX}); Q27 (*red*, *square*), K49 (*triangle*, *blue*), G59 (*circle*, *green*), and F73 (*diamond*, *pink*). The *solid lines* connecting the points are the fits obtained using the modified Gibbs–Helmholtz equation (Eq. 8)

at higher temperatures, they do not have sufficient data points to fit to Eq. (8). Whereas, residues E30, K31, D37, Y50, G63, Y65 and R71 are having very fast decay rates resulting in insufficient number of points (less than 4 points) for fitting. All the fast decaying residues are present at the edges of the structural elements or at the dimer interface.

Discussion

Thermodynamics of unfolding in DLC8 dimer

Residue-specific stability

Recent studies on DLC8 dimer highlighted the sensitivity of dynein light chain protein to small environmental perturbations and suggested that the dimer stability and dynamic modulations across various structural elements play crucial roles in the variety of functions the protein performs (Krishna Mohan and Hosur 2007; Mohan and Hosur 2008a; Song et al. 2007). In order to throw light on the thermal stability of the dimer we obtained the parameters, namely, temperature of maximum conformational stability (T_s) and the free energy of maximum stability ($\Delta G(T_s)$) for all the residues whose unfolding energetics have been calculated. As discussed by Zipp and Kauzmann (1973), Stowell and Rees (1995) the stability curve (ΔG vs. T) can be approximated as a quadratic function of temperature, with the free energy of maximal stability, occurring at a temperature (T_s), given by,

$$\Delta G(T_s) \cong \left[\frac{\Delta H_m^2}{2T_m \Delta C_p}\right] \tag{10}$$

The temperature of maximum conformational stability can be formulated as suggested by Becktel and Schellman (1987)

$$T_s = \frac{T_m}{e^{\left(\Delta H_m / \Delta C_p T_m\right)}} \tag{11}$$

where the individual entities have the same definition as described in earlier sections.

The residue-specific free energy and the temperature of maximum conformational stability thus obtained in DLC8 dimer are given in Table 1 and the summary of the free energies of maximum stability for DLC8 dimer is shown in Fig. 4a. The residue-specific analysis of the temperatures of maximum conformational stability suggests that the values of T_s for all the residues have spanned between 292 and 311 K with an average T_s of 303 K. This value is 10 K higher than that of the T_s value (293.6 K) obtained for DLC8 monomer at pH 3 (Krishna Mohan 2007) indicating that the dimeric molecule is conformationally more stable than its monomeric unit. Further, to correlate the residue-specific stabilities with their location on the dimeric structure, we have marked the residues on the native structure of the protein in Fig. 4b with different color coding. It is evident that the stability index varies significantly among the various structural elements. Among the antiparallel β-sheets β1 and β3 strands which are solvent exposed are least protected and hence least stabilized. Among the remaining β-sheets, β4 strand is more stable compared to β2 and the β5 strand is observed to be the most stable among all the β-sheets as several residues (I83, L84 and F86) did not exchange even at higher temperatures (303 K) even up to several months. It is interesting to note that the stability features between the two helices are significantly different. The stability of the α2-helix increases towards the centre.

Next, to identify the residues contributing maximally to the global stability of the dimeric molecule we compared the free energies of the individual residues obtained here with those obtained from GdnHCl denaturation experiments. Although the two unfolding transitions generated by heat and GdnHCl are entirely different, the free energy change that represents the two unfolding transitions must be expected to be the same as the end points are likely to be the same (Kamal et al. 2002). It is worth noting that the GdnHCl induced dimer unfolding has two transitions; the first transition corresponds to dimer dissociation and the second transition corresponds to unfolding of the monomers (Barbar et al. 2001; Mohan et al. 2009b). Further, the presence of monomeric intermediate has also been identified in the equilibrium folding transition (Mohan et al.

Table 1 Summary of the thermodynamic parameters obtained for the individual residues using temperature dependent HX

Residue	Position	ΔH_m (kcal/mol)	ΔT_m(K)	ΔC_p (kcal/mol^{-1}K^{-1})	T_s (K)	$\Delta G(T_s)$ (kcal/mol)
Q 18	α1 helix	95.8 ± 8.0	358 ± 4.5	1.5 ± 0.2	300	8.4
Q19	α1 helix	73.3 ± 6.5	363 ± 5.3	1.1 ± 0.2	303	6.7
D 20	α1 helix	95.9 ± 9.8	350 ± 4.4	1.9 ± 0.4	303	6.9
A 21	α1 helix	125.1 ± 11.1	351 ± 4.6	2.1 ± 0.5	297	10.6
V 22	α1 helix	139.5 ± 10.5	345 ± 3.8	3.0 ± 0.6	301	9.4
D 23	α1 helix	84.2 ± 8.6	364 ± 6.1	1.3 ± 0.3	306	7.3
C 24	α1 helix	118.5 ± 10.2	357 ± 5.5	2.0 ± 0.4	303	9.6
A25	α1 helix	274.2 ± 14.9	327 ± 1.7	9.1 ± 0.7	302	11.7
T26	α1 helix	118.3 ± 9.9	355 ± 5.0	2.1 ± 0.4	303	9.5
Q27	α1 helix	80.2 ± 7.5	368 ± 6.4	1.2 ± 0.2	311	7.0
A28	α1 helix	91.6 ± 7.6	366 ± 5.7	1.3 ± 0.3	302	8.8
L29	α1 helix	127.2 ± 9	348 ± 4.6	2.7 ± 0.3	298	8.5
Y32	α1–α2 loop	72.7 ± 6.9	336 ± 6.4	1.7 ± 0.3	297	4.6
I 38	α2 helix	116.3 ± 4.9	340 ± 1.4	3.3 ± 0.3	307	7.0
A39	α2 helix	122.4 ± 6.9	351 ± 3.7	2.4 ± 0.4	304	8.7
A40	α2 helix	122.8 ± 7.6	352 ± 2.2	2.4 ± 0.5	305	8.8
Y41	α2 helix	130.2 ± 5.9	349 ± 1.0	2.6 ± 0.2	303	9.2
I42	α2 helix	189.9 ± 12.8	337 ± 4.1	5.2 ± 0.7	302	10.6
K43	α2 helix	200.6 ± 13.5	336 ± 2.5	5.6 ± 0.6	301	10.8
E45	α2 helix	140.7 ± 2.6	341 ± 0.6	3.0 ± 0.1	298	9.7
F46	α2 helix	259.2 ± 12.1	335 ± 1.3	8.2 ± 0.6	305	11.0
D47	α2 helix	107 ± 16.4	356 ± 5.8	1.4 ± 0.2	296	11.7
K48	α2 helix	114.8 ± 6.6	354 ± 3.4	2.1 ± 0.2	303	9.0
K49	α2 helix	91.6 ± 7.0	361 ± 4.2	1.7 ± 0.3	309	7.0
W54	β2 sheet	99.4 ± 7.2	353 ± 4.6	2.0 ± 0.3	306	7.2
C56	β2 sheet	73.0 ± 4.4	358 ± 5.3	1.0 ± 0.1	292	7.5
V58	β2 sheet	96.0 ± 4.6	345 ± 2.0	2.4 ± 0.2	308	5.5
G59	β2 sheet	84.6 ± 4.2	363 ± 3.4	1.4 ± 0.1	306	7.2
F73	β4 sheet	97.5 ± 5.7	356 ± 3.7	1.7 ± 0.2	303	7.9
I74	β4 sheet	152.6 ± 11.2	347 ± 3.8	3.3 ± 0.5	303	10.5
Y75	β4 sheet	129.3 ± 7.2	348 ± 5.2	2.7 ± 0.4	304	8.9
F76	β4 sheet	203.3 ± 21.9	337 ± 3.5	5.5 ± 0.8	303	11.1
Y77	β4 sheet	103.5 ± 8.7	357 ± 5.7	1.8 ± 0.3	303	8.5
L78	β4 sheet	71.8 ± 7.5	366 ± 4.3	1.1 ± 0.2	304	6.6
V81	β5 sheet	51.9 ± 7.6	344 ± 4.4	1.0 ± 0.4	293	4.1
A82	β5 sheet	82.1 ± 6.7	370 ± 5.7	1.0 ± 0.2	303	9.3
L85	β5 sheet	142.2 ± 11.9	351 ± 4.0	2.8 ± 0.5	304	10.4

2009b). As the H-D exchange happens from the open conformation resulting from local or global unfolding of the dimer, we used the free energy value obtained by CD ($\Delta G = 10.4$ kcal/mol) as a reference for global stability of the dimer molecule (Mohan et al. 2009a). This value is represented in the Fig. 4a as a horizontal solid line. Figure 4a and c show that residues ($\Delta G(T_s) > 10.4$ kcal/mol) contributing substantially to the global stability of the molecule belong to different structural elements. These residues are marked with red on the native structure in Fig. 4b. It is evident that residues belonging to the α2-helix and the β5-strand contribute significantly, followed by some residues in the α1-helix and the β4-strand (Fig. 4c). Further a closer examination of the data in the background of the crystal structure of the dimer (Liang et al. 1999) revealed that most of the residues that impart stability are hydrophobic in nature, form the core of monomeric subunit of the dimer and are surrounded by the side chain aromatic rings of Phe and Tyr residues. The packing of all these residues is shown in Fig. 4d. Clearly, the figure depicts that although these stabilizing residues are far away in the primary sequence they are very closely clustered (several

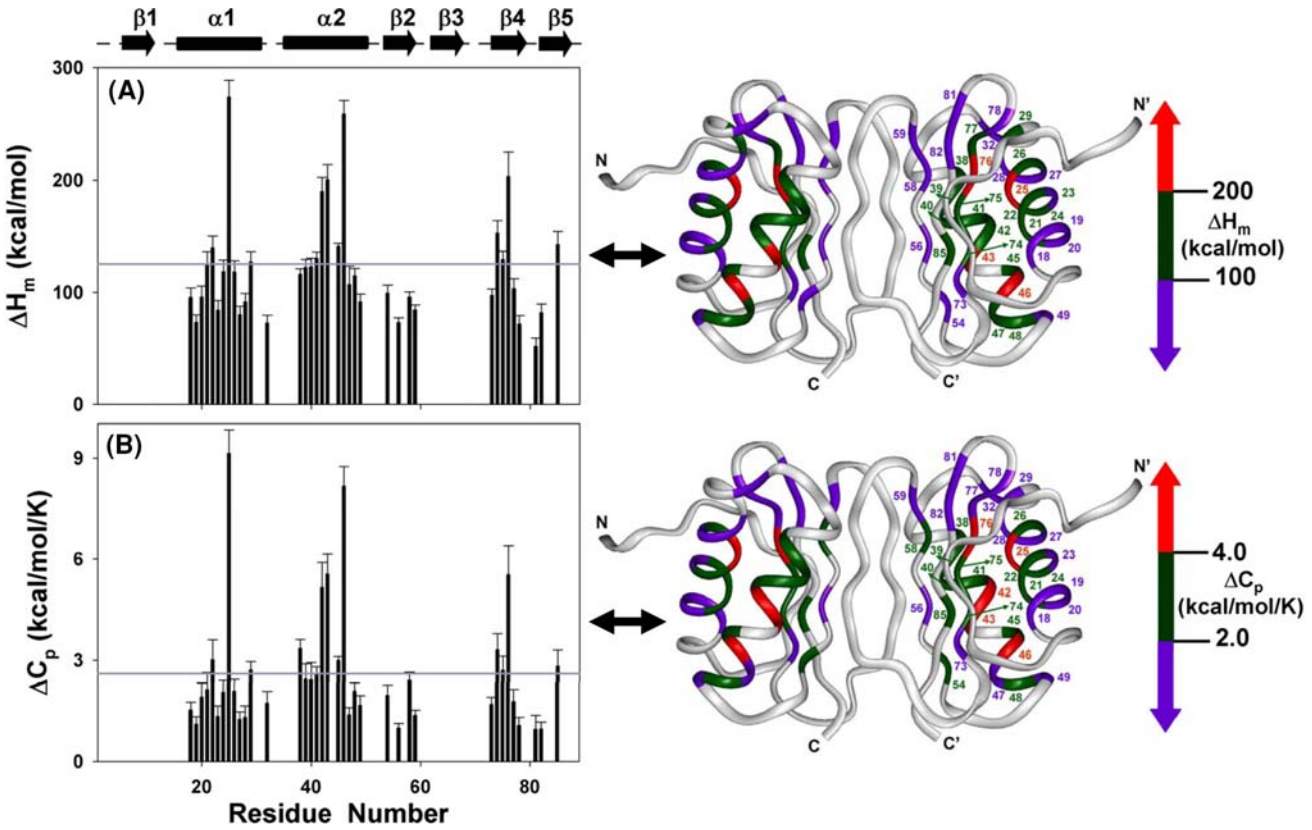

Fig. 3 **a** Enthalpy at the midpoint of transition (ΔH_m) and **b** change in heat capacity (ΔC_p) plotted against the residue number (see Table 1). The secondary structural elements in the protein are marked above with *cylinders* (for helices) and *arrows* (for sheets). The *horizontal solid line* in **a** and **b** represents the average value. The adjacent structures (PDB ID: 1f3c) display summary of the enthalpy at the midpoint of transition (ΔH_m) and change in heat capacity (ΔC_p) shown in the *left panels*; gradient coloring (*violet* → *green* → *red*) is used to show the differences in the unfolding energetics at different segments of the molecule. *Numbers* for all the *colored* residues are annotated on one of the monomers only for better clarity. The primed and the unprimed labels distinguish the two monomers. The images were produced using Insight II

side chain atoms within 3–5 Å distance) in the native topology of the dimer with strong H-bonding networks between the backbone atoms.

Unfolding characteristics of DLC8 dimer

Thermodynamic analysis of DLC8 dimer revealed several interesting features. We observed a great dispersion in the obtained T_m values among the individual residues i.e., a dispersion of 35 K (from 335 to 370 K) with an average value of 355 K. This indicates that the thermal unfolding transition of DLC8 dimer is broad. It is worth noting that the average T_m obtained for the dimer is 13 K greater than that of the T_m (343 K) for DLC8 monomer at pH 3 (Krishna Mohan 2007). This implies that the dimer is thermally more stable than its monomeric counterpart. Further, greater degree of variation has been noticed in the different structural elements in all the measured thermodynamic parameters (enthalpy at midpoint of transition and heat capacity changes) (Fig. 3), which suggested differential stability among the various segments of the molecule. The data in Table 1 reveals an interesting cooperative unit of unfolding in the α2 helix; residues A39, A40 and Y41 (Fig. 5) have similar values of T_m, ΔH_m and ΔC_p. Other than these there is a substantial variation in the values of the parameters in all the structured elements of the protein. Thus, we conclude that the thermal unfolding of DLC8 dimer is not a simple two state unfolding process, but is complex, possibly comprising of differently unfolded intermediates in the equilibrium unfolding transition.

Comparison of thermal and denaturant induced unfolding features

Recently, we investigated the ruggedness of the energy landscape of DLC8 dimer using HX in the presence of guanidine hydrochloride (GdnHCl) (Mohan et al. 2009a) at sub-denaturing concentrations. Comparison of the results obtained in the present study with those of the denaturant dependent HX study provided valuable insights into the overall global stability and unfolding features of the dimeric molecule. We observed several common features

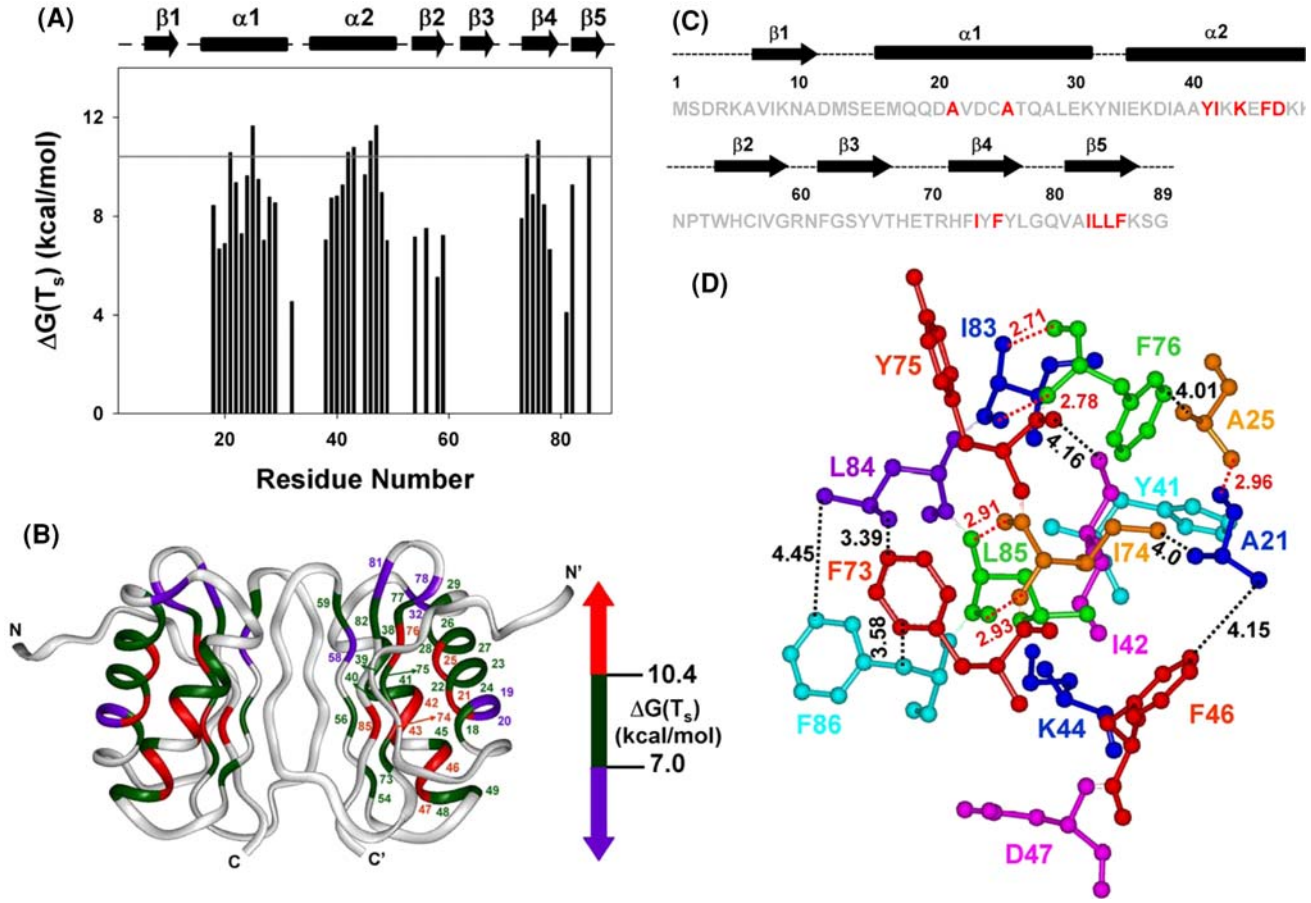

Fig. 4 **a** Summary of the free energy of maximum stability for the individual residues of DLC8 dimer at pH 7 (see Table 1). The secondary structural elements in the protein are marked above with *cylinders* (for helices) and *arrows* (for sheets). **b** The free energy of maximum stability $\Delta G(T_s)$ shown in '**a**' are marked on the native structure with gradient coloring (*violet* → *green* → *red*) to show the differences in stability at different segments of the molecule. *Numbers* for all the *colored* residues are indicated on one of the monomers only for better clarity. The primed and the unprimed labels distinguish the two monomers. **c** Residues with free energy of maximum stability >10.4 kcal/mol are marked with red on the primary sequence of DLC8 dimer. Residues whose peaks did not decay up to 303 K (K44, I83, L84 and F86) are also marked with red on the sequence as they possess very high stabilization energies. The secondary structural elements are also shown on the top of the sequence. **d** Zooming in on a particular region of the interior of one of the monomeric subunit of the DLC8 dimer in the crystal structure (PDB id: 1cmi), to show the interactions of various hydrophobic side chains and backbone H-bonding network. H-bonds across some of the residues are marked with *dotted red lines*. Some of the side chain atoms which are at a distance of 3–5 Å are marked with dotted black line in order to illustrate the proximity of these residues in the native structure. The images 4**b** and **d** were produced using Insight II

between the thermal and GdnHCl induced unfolding energetics. The differential stability of the various segments in the dimeric molecule is almost conserved in both measurements. It is interesting to note that the thermodynamic parameters obtained for the residues A25, F46, D47, I74 and F76 in both denaturation studies correlate well with the values of the energetic parameters of the global unfolding phenomenon indicating that these ones contribute significantly to the global stability of the DLC8 dimer. Further, several of the residues which have been identified to unfold via local fluctuations in the GdnHCl study show comparatively lower values of enthalpy at midpoint of transition (<100 kcal/mol) and smaller values of heat capacity changes (<1.5 kcal/mol^{-1}K^{-1}) suggesting minimal contribution of these residues to the global stability of the dimer. Moreover, the small cooperative unfolding segment (A39–Y41) in the α2 helix seen here is also seen during the unfolding studies by different means. It is always debated in the literature that the *m*-values obtained in the denaturant dependent unfolding and the ΔC_p values obtained during the thermal denaturation should go hand in hand as both the parameters reflect the burial of nonpolar groups. Indeed, it is worth noting that we observed a strong correlation between these two parameters. We observed higher values of ΔC_p for the residues that exhibited higher *m-values* (A25, F46 and F76 etc.) and vice versa. All these facts establish that both temperature dependent and denaturant dependent HX studies report

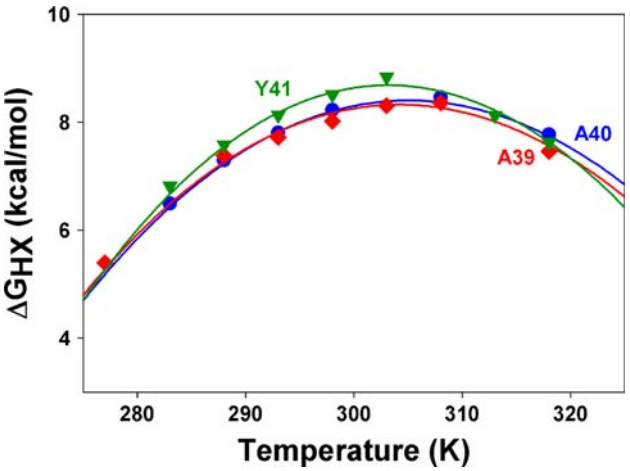

Fig. 5 Plots of temperature dependence of stabilization free energies (ΔG_{HX}) for the backbone amide protons which have similar enthalpy at the midpoint of transition (ΔH_m) and change in heat capacity (ΔC_p) and temperature at transition mid point T_m (see Table 1); A39 (*diamond*, *red*), A40 (*circle*, *blue*), and Y41 (*Triangle*, *green*). The *solid lines* connecting the points are the fits obtained using the modified Gibbs–Helmholtz equation (Eq. 8)

similarly on the energy landscape of DLC8 dimer to be rugged, populated by intermediates along the unfolding transition.

Conclusions

In conclusion, the study suggested that the various segments of DLC8 dimer have different stabilities. It is also evident that the equilibrium thermal unfolding is not a simple two state transition, but comprises of intermediates. Further, the study indicated that the dimeric species is thermally and conformationally more stable than its monomeric counterpart. A good agreement has been observed between the thermodynamic parameters obtained by using temperature dependent and denaturant dependent hydrogen exchange studies indicating that the segments contributing to the global stability of the dimeric protein in both cases are similar. Thus, these results demonstrate that the sequence and structure of the protein indeed can dictate the unfolding characteristics of the protein. All these results provide valuable insights into the stability features and ruggedness of the energy landscape of DLC8 dimer and reflect on the plasticities of the various segments of the protein. These findings have great implications for the adaptability of the protein (DLC8 dimer acts as a cargo adaptor in dynein motor complex) to bind different targets which could have different structures and flexibilities.

Acknowledgments We thank Government of India for providing financial support to the National Facility for High Field NMR at the Tata Institute of Fundamental Research. The authors acknowledge Dr. Anindya Ghosh-Roy for the DLC8 clone, Dr. M. M. G Krishna for HX Excel spread sheet, and Dr. Sulakshana Mukherjee for critical comments. PMKM is a recipient of TIFR Alumni Association Scholarship (2003–2005) and Sarojini Damodaran International Fellowship for career development, supported by the TIFR endowment fund.

References

Bai Y, Milne JS, Mayne L, Englander SW (1993) Primary structure effects on peptide group hydrogen exchange. Proteins 17:75–86

Bai Y, Milne JS, Mayne L, Englander SW (1994) Protein stability parameters measured by hydrogen exchange. Proteins 20:4–14

Bai Y, Sosnick TR, Mayne L, Englander SW (1995) Protein folding intermediates: native-state hydrogen exchange. Science 269: 192–197

Barbar E, Kleinman B, Imhoff D, Li M, Hays TS, Hare M (2001) Dimerization and folding of LC8, a highly conserved light chain of cytoplasmic dynein. Biochemistry 40:1596–1605

Becktel WJ, Schellman JA (1987) Protein stability curves. Biopolymers 26:1859–1877

Brorsson AC, Kjellson A, Aronsson G, Sethson I, Hambraeus C, Jonsson BH (2004) The "two-state folder" MerP forms partially unfolded structures that show temperature dependent hydrogen exchange. J Mol Biol 340:333–344

Chamberlain AK, Marqusee S (1997) Touring the landscapes: partially folded proteins examined by hydrogen exchange. Structure 5:859–863

Chi YH, Kumar TK, Chiu IM, Yu C (2002) Identification of rare partially unfolded states in equilibrium with the native conformation in an all beta-barrel protein. J Biol Chem 277:34941–34948

Chu R, Pei W, Takei J, Bai Y (2002) Relationship between the native-state hydrogen exchange and folding pathways of a four-helix bundle protein. Biochemistry 41:7998–8003

Dill KA (1990) Dominant forces in protein folding. Biochemistry 29:7133–7155

Dyson HJ, Wright PE (1996) Insights into protein folding from NMR. Annu Rev Phys Chem 47:369–395

Fuhrmann JC, Kins S, Rostaing P, El FO, Kirsch J, Sheng M, Triller A, Betz H, Kneussel M (2002) Gephyrin interacts with Dynein light chains 1 and 2, components of motor protein complexes. J Neurosci 22:5393–5402

Hoang L, Bedard S, Krishna MM, Lin Y, Englander SW (2002) Cytochrome c folding pathway: kinetic native-state hydrogen exchange. Proc Natl Acad Sci USA 99:12173–12178

Honig B (1999) Protein folding: from the levinthal paradox to structure prediction. J Mol Biol 293:283–293

Hvidt A, Nielsen SO (1966) Hydrogen exchange in proteins. Adv Protein Chem 21:287–386

Jaffrey SR, Snyder SH (1996) PIN: an associated protein inhibitor of neuronal nitric oxide synthase. Science 274:774–777

Kamal JK, Nazeerunnisa M, Behere DV (2002) Thermal unfolding of soybean peroxidase. Appropriate high denaturant concentrations induce cooperativity allowing the correct measurement of thermodynamic parameters. J Biol Chem 277:40717–40721

Kauzmann W (1959) Some factors in the interpretation of protein denaturation. Adv Protein Chem 14:1–63

Krishna Mohan PM (2007) Unfolding energetics and conformational stability of DLC8 monomer. Biochimie 89:1409–1415

Krishna Mohan PM, Hosur RV (2007) NMR insights into dynamics regulated target binding of DLC8 dimer. Biochem Biophys Res Commun 355:950–955

Krishna Mohan PM, Barve M, Chatterjee A, Ghosh-Roy A, Hosur RV (2008) NMR comparison of the native energy landscapes of DLC8 dimer and monomer. Biophys Chem 134:10–19

Krishna MM, Hoang L, Lin Y, Englander SW (2004) Hydrogen exchange methods to study protein folding. Methods 34:51–64

Liang J, Jaffrey SR, Guo W, Snyder SH, Clardy J (1999) Structure of the PIN/LC8 dimer with a bound peptide. Nat Struct Biol 6: 735–740

Linderstrøm-Lang K (1958) Deuterium exchange and protein structure. In: Neuberger (ed) Symposium on protein structure, London

Lo KW, Kan HM, Chan LN, Xu WG, Wang KP, Wu Z, Sheng M, Zhang M (2005) The 8-kDa dynein light chain binds to p53-binding protein 1 and mediates DNA damage-induced p53 nuclear accumulation. J Biol Chem 280:8172–8179

Lopez MM, Makhatadze GI (2002) Differential scanning calorimetry. Methods Mol Biol 173:113–119

Maity H, Maity M, Krishna MM, Mayne L, Englander SW (2005) Protein folding: the stepwise assembly of foldon units. Proc Natl Acad Sci USA 102:4741–4746

Mohan PM, Hosur RV (2008a) NMR characterization of structural and dynamics perturbations due to a single point mutation in Drosophila DLC8 dimer: functional implications. Biochemistry 47:6251–6259

Mohan PM, Hosur RV (2008b) pH dependent unfolding characteristics of DLC8 dimer: residue level details from NMR. Biochim Biophys Acta 1784:1795–1803

Mohan PM, Barve M, Chatterjee A, Hosur RV (2006) pH driven conformational dynamics and dimer-to-monomer transition in DLC8. Protein Sci 15:335–342

Mohan PM, Chakraborty S, Hosur RV (2009a) Residue-wise conformational stability of DLC8 dimer from native-state hydrogen exchange. Proteins 75(1):40–52

Mohan PM, Joshi MV, Hosur RV (2009b) Hierarchy in guanidine unfolding of DLC8 dimer: regulatory functional implications. Biochimie 91(3):401–407

Mukherjee S, Mohan PM, Kuchroo K, Chary KV (2007) Energetics of the native energy landscape of a two-domain calcium sensor protein: distinct folding features of the two domains. Biochemistry 46:9911–9919

Pace CN (1975) The stability of globular proteins. CRC Crit Rev Biochem 3:1–43

Pace CN (1986) Determination and analysis of urea and guanidine hydrochloride denaturation curves. Methods Enzymol 131: 266–280

Pace CN, Shirley BA, McNutt M, Gajiwala K (1996) Forces contributing to the conformational stability of proteins. FASEB J 10:75–83

Privalov PL, Khechinashvili NN (1974) A thermodynamic approach to the problem of stabilization of globular protein structure: a calorimetric study. J Mol Biol 86:665–684

Puthalakath H, Villunger A, O'Reilly LA, Beaumont JG, Coultas L, Cheney RE, Huang DC, Strasser A (2001) Bmf: a proapoptotic BH3-only protein regulated by interaction with the myosin V actin motor complex, activated by anoikis. Science 293: 1829–1832

Rose GD, Wolfenden R (1993) Hydrogen bonding, hydrophobicity, packing, and protein folding. Annu Rev Biophys Biomol Struct 22:381–415

Rumbley J, Hoang L, Mayne L, Englander SW (2001) An amino acid code for protein folding. Proc Natl Acad Sci USA 98:105–112

Shih P, Holland DR, Kirsch JF (1995) Thermal stability determinants of chicken egg-white lysozyme core mutants: hydrophobicity, packing volume, and conserved buried water molecules. Protein Sci 4:2050–2062

Song Y, Benison G, Nyarko A, Hays TS, Barbar E (2007) Potential role for phosphorylation in differential regulation of the assembly of dynein light chains. J Biol Chem 282:17272–17279

Stowell MH, Rees DC (1995) Structure and stability of membrane proteins. Adv Protein Chem 46:279–311

Vadlamudi RK, Bagheri-Yarmand R, Yang Z, Balasenthil S, Nguyen D, Sahin AA, den HP, Kumar R (2004) Dynein light chain 1, a p21-activated kinase 1-interacting substrate, promotes cancerous phenotypes. Cancer Cell 5:575–585

Zipp A, Kauzmann W (1973) Pressure denaturation of metmyoglobin. Biochemistry 12:4217–4228